

Atomic Force Microscopy Study of Clay Nanoplatelets and Their Impurities

Richard D. Piner, Terry T. Xu, Frank T. Fisher, Yi Qiao, and Rodney S. Ruoff*

Department of Mechanical Engineering, Northwestern University, Evanston, Illinois 60208

Received May 7, 2003. In Final Form: July 1, 2003

The results of an in-depth study of 1 nm thick individual clay sheets by atomic force microscopy (AFM) are presented. Several techniques have been employed, including lateral force microscopy (LFM) and force modulation microscopy (FMM). The individual clay sheets, also referred to as clay nanoplatelets in the literature, were found to be extremely compliant and strongly adhered to a variety of substrates. In all cases, these nanoplatelets were accompanied by mobile impurities that could not be separated from the nanoplatelets. A detailed examination of these impurities using AFM suggests that they are comprised of low molecular weight silicates as well as the intercalating salt used to process the clay. An understanding of the nature and chemistry of these impurities will be necessary as models of these clays are developed for various applications, such as reinforcement in composite materials or elements for molecular electronics. Further, these clay nanoplatelets and their impurities present a novel two-dimensional nanoscale system for future surface science studies using AFM and other methods.

Introduction

The term “clay” refers to a class of materials generally made up of layered silicates that are similar to mica. While these clay particles can span centimeters in lateral dimensions, the in-plane dimensions of the individual clay layers are on the order of a micron, and the thickness of a single clay nanoplatelet is on the order of a nanometer. These layered clays are characterized by strong intralayer covalent bonds within the individual sheets comprising the clay, with only weak van der Waals interactions between adjacent clay sheets. These strong in-plane covalent bonds have generated significant interest in the use of these materials as a reinforcing element in composite materials. However, because of the weak interaction between adjacent clay sheets, a significant effort on clay-reinforced polymers has focused on methods of intercalating the polymer within the intralayer galleries, or completely exfoliating the clays so that individual clay sheets are dispersed within the polymer, to maximize the contact area (and hence the interaction) between the polymer and the clay. Brillouin scattering measurements on bulk muscovite mica give in-plane moduli on the order of 170 GPa, while the modulus perpendicular to the layers is given as about 60 GPa.¹ Experimental measurements on clay particles give a much lower modulus value in the *C*-direction.² However, we are unaware of experiments that have attempted to measure the modulus of an individual clay nanoplatelet. Thus, the motivation of the current work was to probe the mechanical properties of individual clay nanoplatelets using AFM.

The interest in using clay as a reinforcing phase in a polymer matrix composite was spurred by the pioneering work by researchers at Toyota in the early 1990s.^{3–5} Since

that time, research into clay nanocomposites has exploded; the reader is referred to recent review articles for an in-depth discussion of the current state of the art.^{6–13} In general, the incorporation of the nanoclays into various polymers has been shown to result in increases in tensile properties (elastic modulus, tensile strength), decreased thermal expansion coefficients and improved thermal stability, increased swelling resistance, decreased gas permeability, and improved flammability properties. A new class of nanoclay–polymer composites, based on the layer-by-layer assembly of individual clay nanoplatelets and appropriate polymers, is also under development.^{14–17} Because of the large surface area of the clay nanoplatelets within the nanocomposite, an understanding and control of the clay surface are expected to play an important role in the optimization of these material systems. Models of the mechanical properties of the individual clay nanoplatelets, as input parameters into models of effective clay nanocomposite behavior, will also be critical.

However, these clay nanoplatelets are interesting above and beyond their use as an element of composite materials. Because the individual clay platelet thicknesses are on the order of 1 nm, with lateral dimensions on the micron

(5) Kojima, Y.; Usuki, A.; Kawasumi, M.; Okada, A.; Kurauchi, T.; Kamigaito, O.; Kaji, K. *J. Polym. Sci., Part B: Polym. Phys.* **1995**, *33*, 1039.

(6) Biswas, M.; Ray, S. S. In *New Polymerization Techniques and Synthetic Methodologies*; Springer-Verlag: Berlin, 2001.

(7) LeBaron, P. C.; Wang, Z.; Pinnavaia, T. J. *Appl. Clay Sci.* **1999**, *15*, 11.

(8) Schmidt, D.; Shah, D.; Giannelis, E. P. *Curr. Opin. Solid State Mater. Sci.* **2002**, *6*, 205.

(9) Alexandre, M.; Dubois, P. *Mater. Sci. Eng., R* **2000**, *28*, 1.

(10) Schulz, J. C.; Warr, G. G. *Langmuir* **2002**, *18*, 3191.

(11) Vaia, R. A.; Giannelis, E. P. *MRS Bull.* **2001**, *26*, 394.

(12) Carrado, K. A. In *Advanced Polymeric Materials: Structure Property Relationships*; Advani, S. G., Shonaike, G. O., Eds.; CRC Press LLC: Boca Raton, FL, 2003.

(13) Pinnavaia, T. J.; Beall, G. Eds. *Polymer-Clay Nanocomposites*; Wiley & Sons: Chichester, UK, 2000.

(14) Zhou, Y. L.; Li, Z.; Hu, N. F.; Zeng, Y. H.; Rusling, J. F. *Langmuir* **2002**, *18*, 8573.

(15) Fan, X.; Park, M.; Xia, C.; Advincula, R. *J. Mater. Res.* **2002**, *17*, 1622.

(16) Mamedov, A.; Ostrander, J.; Aliev, F.; Kotov, N. A. *Langmuir* **2000**, *16*, 3941.

(17) Tang, Z.; Kotov, N. A.; Magonov, S.; Ozturk, B. *Nature Mater.* **2003**, *2*, 413.

* To whom all correspondence should be addressed: Tel (847) 467-6596; Fax (847) 491-3915; e-mail r-ruoff@northwestern.edu.

(1) McNeil, L. E.; Grimsditch, M. *J. Phys.: Condens. Matter* **1993**, *5*, 1681.

(2) Prasad, M.; Kopycinska, M.; Rabe, U.; Arnold, W. *Geophys. Res. Lett.* **2002**, *29*, 1172.

(3) Kojima, Y.; Usuki, A.; Kawasumi, M.; Okada, A.; Kurauchi, T.; Kamigaito, O. *J. Polym. Sci., Polym. Chem.* **1993**, *31*, 983.

(4) Kojima, Y.; Usuki, A.; Kawasumi, M.; Okada, A.; Kurauchi, T.; Kamigaito, O.; Kaji, K. *J. Polym. Sci., Part B: Polym. Phys.* **1994**, *32*, 625.

Table 1. Clay Samples Studied in This Work

name	mineral type	supplier
cloisite Na+	sodium montmorillonite	Southern Clay Products
lithium fluorohectorite	Li + FH ^a	Corning
SOMASIF ME-100f	sodium synthetic flouromica	UniCoOp
SOMASIF ME-300	sodium synthetic flouromica	UniCoOp

^a No longer available.

scale, they are the two-dimensional analogue of zero-dimensional (quantum dots, nanoclusters) and one-dimensional (nanotube, nanowires) materials. In addition, depending on their thermal and electrical properties, the silicate nanoplatelets are a potential building block for nanoscopic electrical devices. The presence of impurities associated with the clay nanoplatelets, and the inability to separate these nanoplatelets from the impurities, complicate the surface chemistry of these materials.^{18,19} Unless methods are found for their removal, these impurities will prevent accurate measurements of the mechanical, electrical, and thermal properties of the individual clay nanoplatelets.

Experimental Section

Reagent grade chemicals were used as delivered. Tetrahydrofuran (THF), acetonitrile (ACN), *N,N*-dimethylformamide (DMF), and dodecylamine were from Aldrich. 3-Aminopropyltriethoxysilane was from Alfa-Aesar, and toluene was from Fisher. Water was purified using a Barnstead model D6431 three-cartridge filter system. Mica substrates were from Ted Pella, and highly ordered pyrolytic graphite (HOPG) was from SPI. Gold films were deposited with an Edwards model 306 e-beam evaporation system. Ultrasonication was done using a Crest model 175HT, 50 W bath.

Clay Characterization. All images were recorded on Park Scientific model CP Research AFMs. Contact mode images were made with Park Scientific microlevers with silicon nitride tips. Tapping mode images were made with Park Scientific noncontact ultralevers with silicon tips. (Note that Park Scientific is now owned by Veeco.) Typical scan speeds were 1 or 2 Hz. The contact mode set point was for a normal force of 1 nN. In tapping mode, the resonant frequency was about 90 kHz, with small variations from cantilever to cantilever. Time-of-flight secondary ion mass spectrometry (TOF-SIMS) was performed using a Physical Electronics model Thrift III.

Processing of Clays. A number of different clays samples were examined in this work (see Table 1). Other than details of lateral dimensions, all clays looked very similar by AFM. The exfoliation, mechanical behavior, and presence of impurities also appeared to be similar for all samples. Thus, our efforts focused on the SOMASIF ME-300 sample, a "synthetic" clay made from natural talc. According to the manufacturer (UniCoOP, Tokyo, Japan), the clay is processed by heating talc in the presence of Na₂SiF₆, such that the salt decomposes and the Na ions intercalate between the silicate layers that comprise the talc. When placed in water and agitated, water can enter the galleries and further swell the talc until it becomes completely exfoliated.

To study individual clay nanoplatelets via AFM, it is necessary to first fully exfoliate the clay crystals, followed by deposition on a suitable substrate. Unless otherwise specified in the text, the individual clay nanoplatelets were prepared in the following manner. First, a few micrograms of the clay powder was placed in 10 mL of pure water. The clays were exfoliated in a low-power ultrasonic bath for 8–16 h. After this, the resulting suspension was allowed to settle for a day or more. Sedimentation allows the

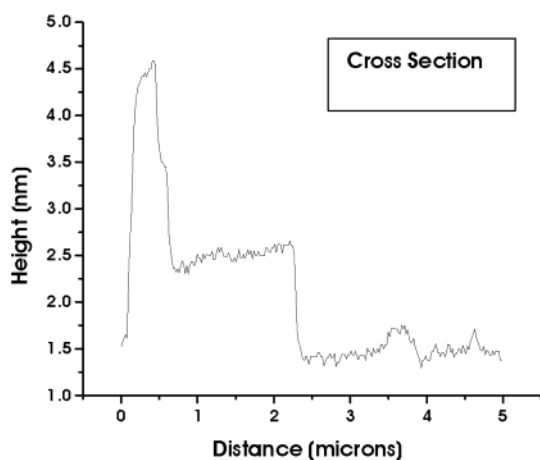


Figure 1. Five micron square topography scan of 1 nm high individual clay nanoplatelets. The height profile is marked by the line drawn on the topography image.

nonexfoliated clays to sink, while the fully exfoliated individual clay sheets will stay in suspension for months. A drop of the suspension is then placed on a substrate and allowed to stand for a few minutes. The excess water is then removed by a high-velocity jet of compressed gas or is wicked away. Clay nanoplatelet coverage on a substrate can be controlled by adjusting the concentration of the suspension and the time it is exposed to the substrate.

Results and Discussion

Initial Measurements of Individual Clay Nanoplatelets. Initial AFM images were obtained by depositing the clay nanoplatelets on mica. Mica is ideal for this initial imaging because it is atomically flat and adds nothing to the topology of the system, making it easier to understand the topological features of the clay nanoplatelets. Through trial and error, it was possible to get nanoplatelets evenly distributed in submonolayer coverage on the mica surface. One can distinguish individual clay nanoplatelets by their thickness, as they are 1 nm high in all AFM topography images as shown in Figure 1. Areas where multiple clay nanoplatelets are stacked on top of each other are also visible in the image.

For these initial images of the nanoplatelets, contact mode AFM was used in parallel with lateral force microscopy (LFM). Because LFM is very sensitive to differences in the chemistry of the surface, it would indicate any differences in chemistry between the clays and the mica substrate. This is mostly due to the effects of capillary

(18) Thomas, S. M.; Bertrand, J. A.; Occelli, M. L.; Stencel, J. M.; Gould, S. A. C. *Chem. Mater.* **1999**, *11*, 1153.

(19) Occelli, M. L.; Huggins, F. E.; Dominguez, J. M.; Stencel, J. M.; Gould, S. A. C. *Microporous Mater.* **1995**, *4*, 291.

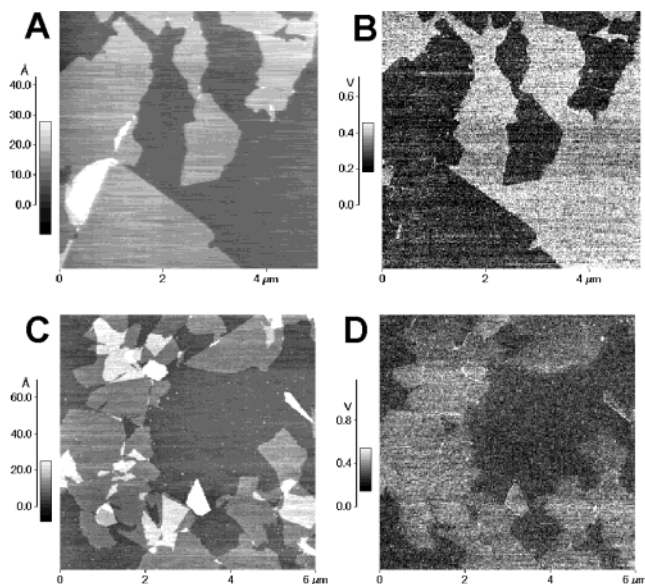


Figure 2. AFM and LFM images of clay nanoplatelet samples on mica directly after deposition (top) and 5 days after deposition (bottom). (A) and (C) are contact mode images of the topology. (B) and (D) are LFM images, where lighter shades indicate higher friction.

forces and the amount of adsorbed water on a sample surface.^{20–23} AFM and LFM images of a clay nanoplatelet sample directly after deposition, and 5 days after deposition, on mica are shown in Figure 2. While the surface topology of the clay samples remains unchanged, the lateral force contrast has reversed over a period of days (i.e., the clay nanoplatelets are light and dark respectively in parts B and D of Figure 1). We believe (see discussion below) that this change in lateral force contrast was due to the migration of impurities. At room temperature these impurities are highly mobile and strongly interact with the AFM tip. In later experiments, it was discovered that this change in contrast can be reversed by rinsing in water, such that the friction on the clay nanoplatelets returns to being lower than on the mica substrate. If the sample is then dried by heating in an oven or by rinsing in ethanol, the contrast again reverses so that friction on the nanoplatelets is higher than the mica substrate. However, after repeating this process several times, the friction on the clay nanoplatelets remained higher than on the mica substrate. Currently, we believe that this behavior is due to a redistribution of impurities and their effect on the local wetting properties of the sample. Rinsing does not remove the impurities, which seem to be strongly attracted to both the clay and the mica. However, the impurities are mobile and seem to prefer to locate on the surface of the clay nanoplatelets. After repeated rinsing they are mostly moved to the top of the clays. The presence of these impurities is significant, as they will alter the surface chemistry of the nanoplatelets and are likely to impact the use of fully exfoliated clays in applications.

Compliance of Individual Clay Nanoplatelets.

Disregarding the issue of impurities for the moment, one of the long-term goals of our research is to understand the mechanics of these clay nanoplatelets. Our first approach was to place individual nanoplatelets across a very narrow gap cut into a glass substrate in order to measure the modulus via a force vs displacement curve on a suspended

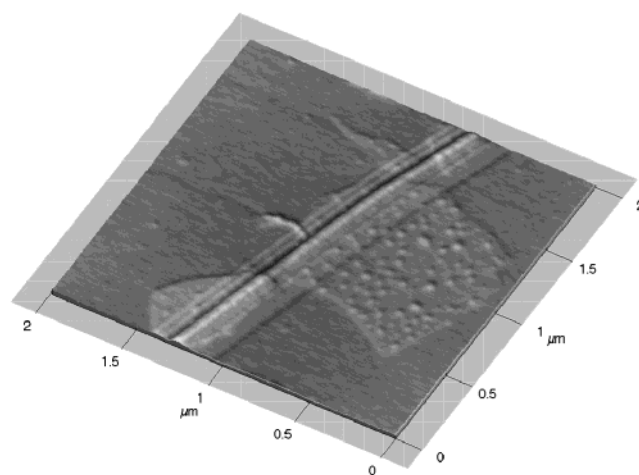


Figure 3. Tapping mode AFM image of an individual clay nanoplatelet conforming to a scratch on glass. The impurities appear as “bumps” on the nanoplatelet.

nanoplatelet. To test this capability, a clay nanoplatelet was deposited across a 100 nm wide scratch in a glass substrate, as shown in Figure 3. Rather than spanning the trench, the clay sinks into the scratch and readily conforms to it. This is consistent with molecular models that show that the clay nanoplatelets should be very compliant in the out-of-plane direction.²⁴

To test whether a smaller gap is necessary for the force vs displacement “drum-skin” test, clay nanoplatelets were deposited on a nanoporous alumina substrate with uniform 60 nm pores spaced 100 nm apart.²⁵ However, similar to our findings with the glass substrate, when placed on a nanoporous alumina substrate the clay nanoplatelets sink into the pores and appear “wrinkled”, as shown in Figure 4. The friction on the clay is lower than the alumina substrate (see Figure 4b), similar to the case for the mica substrate.

Returning to the issue of impurities, initial attempts to separate the impurities from the clay nanoplatelets used an electrophoretic technique. If the nanoplatelets are charged, the application of an electric current might drive the nanoplatelets to one of the gold electrodes and leave any impurities in the water. The electrode was a 20 nm thick polycrystalline gold film evaporated onto mica. These gold electrodes were placed in an aqueous nanoplatelet suspension, and a voltage was applied until a current of about 1 mA could be detected. This method was not successful, as very few nanoplatelets were found on the positive electrode (and none on the negative electrode). A few of the clay nanoplatelets that were found on the positive electrode are shown in Figure 5. Because the individual clay nanoplatelets are so compliant in the out-of-plane direction, the grains of the gold substrate can clearly be seen below the clay plates. The friction is lower on the clay nanoplatelets than on the supporting gold film.

On a few occasions, we observed large areas where the clays formed almost complete monolayers. This may be related to surface charge on the clay nanoplatelets. Under an optical microscope, large rafts of the clays are sometimes seen floating on the surface of the water as a sample is drying, possibly indicating that the nanoplatelets order themselves on the surface of the water and are then left behind as the water film dries. On mica, water dries as a more or less uniform film and does not break up into

(20) Piner, R. D.; Mirkin, C. A. *Langmuir* **1997**, *13*, 6864.

(21) Piner, R. D.; Hong, S.; Mirkin, C. A. *Langmuir* **1999**, *15*, 5457.

(22) Delville, A.; Sokolowski, S. *J. Phys. Chem.* **1993**, *97*, 6261.

(23) Delville, A. *J. Phys. Chem.* **1995**, *99*, 2033.

(24) Sato, H.; Yamagishi, A.; Kawamura, K. *J. Phys. Chem. B* **2001**, *105*, 7990.

(25) Xu, T. T.; Piner, R. D.; Ruoff, R. S. *Langmuir* **2003**, *19*, 1443.

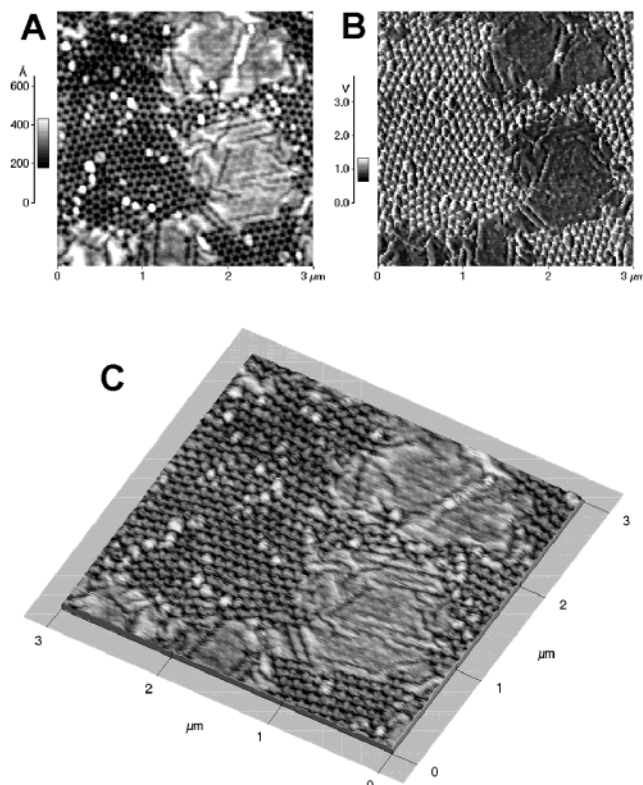


Figure 4. Individual clay nanoplatelets on porous alumina films. (A) is a contact mode topology image, while (B) is the LFM image. In the LFM image, lower friction is darker shade. (C) is a 3D rendering of (A).

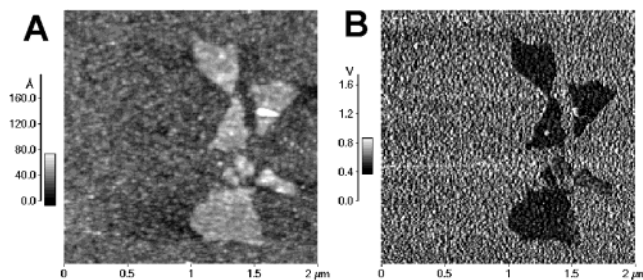


Figure 5. Individual clay nanoplatelets on a gold surface. (A) is contact mode topology, and (B) is the LFM image.

small droplets. A tapping mode AFM image on mica demonstrating this tiling effect is shown in Figure 6.

Force Modulation Microscopy on the Clay Nanoplatelets. As our previous results indicate, the extreme out-of-plane compliance of the individual clay nanoplatelets suggests that meaningful modulus values obtained using a force vs displacement drum-skin test are unlikely. However, there is a new AFM technique known as force modulation microscopy (FMM) that can, in principle, directly measure the modulus of a material at the surface. In FMM, the normal force between the tip and sample is modulated. The amplitude and phase of the response can be used to calculate the contact stiffness of the surface of the sample. In principle, these results can be used to compute the modulus of the sample.^{2,26–34}

(26) Crozier, K. B.; Yaralioglu, G. G.; Degertekin, F. L.; Adams, J. D.; Minne, S. C.; Quate, C. F. *Appl. Phys. Lett.* **2000**, *76*, 1950.

(27) Cuberes, M. T.; Assender, H. E.; Briggs, G. A. D.; Kolosov, O. V. *J. Phys. D: Appl. Phys.* **2000**, *33*, 2347.

(28) Dinelli, F.; Biswas, S. K.; Briggs, G. A. D.; Kolosov, O. V. *Phys. Rev. B* **2000**, *61*, 13995.

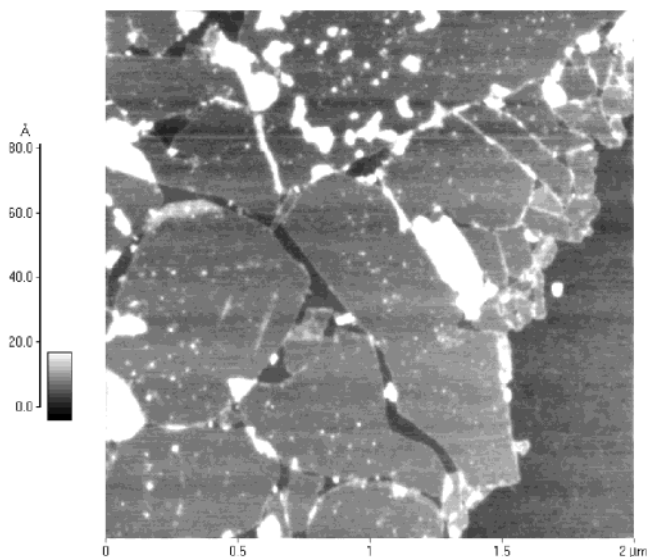


Figure 6. Tapping mode image of many nanoplatelets tiling the mica substrate with only small gaps present in a few locations.

To test whether this new technique is sensitive to the mechanical properties of the clay nanoplatelets, it is necessary to deposit the nanoplatelets on a clean, atomically flat substrate. Clearly, a textured substrate is not suitable for such a technique, as the underlying substrate effects will interfere with measurements on the system under study (see Figure 5). Because mica is a layered silicate and likely has mechanical properties similar to the clays, highly oriented pyrolytic graphite (HOPG) was selected as the substrate. A drop of clay suspension was prepared as described earlier for the mica substrates. However, because HOPG is hydrophobic, the clays did not settle out evenly over the substrate surface. The dynamics of the drying suspension were very different, and the clays tended to pile into large clusters, making it difficult (but not impossible) to find individual nanoplatelets on the substrate. The difference between the individual clay nanoplatelet and the HOPG substrate is quite obvious in the FMM image, as shown in Figure 7. However, Figure 7 also shows that additional material was adsorbed on the substrate. Because the FMM technique is very sensitive to the surface of the sample, any adsorbates could interfere with modulus measurements using this technique.

AFM Analysis of the Clay Impurities. In an attempt to drive off these adsorbates for subsequent FMM analysis, the sample was heated to 100 °C in air for an hour. Because the clays did not settle out evenly over the substrate surface, large clumps of clays were present (not shown) that seem to hold large amounts of the impurity. Over time, the impurity covers the whole HOPG substrate with a thin film, as the impurity is much more mobile on HOPG than on mica. This makes contact mode imaging of the

(29) Dinelli, F.; Castell, M. R.; Ritchie, D. A.; Mason, N. J.; Briggs, G. A. D.; Kolosov, O. V. *Philos. Mag. A: Phys. Condens. Matter Struct. Defect Mech. Prop.* **2000**, *80*, 2299.

(30) Du, B. Y.; Tsui, O. K. C.; Zhang, Q. L.; He, T. B. *Langmuir* **2001**, *17*, 3286.

(31) Iwata, F.; Matsumoto, T.; Sasaki, A. *Nanotechnology* **2000**, *11*, 10.

(32) Kolosov, O. V.; Castell, M. R.; Marsh, C. D.; Briggs, G. A. D.; Kamins, T. I.; Williams, R. S. *Phys. Rev. Lett.* **1998**, *81*, 1046.

(33) McGuigan, A. P.; Huey, B. D.; Briggs, G. A. D.; Kolosov, O. V.; Tsukahara, Y.; Yanaka, M. *Appl. Phys. Lett.* **2002**, *80*, 1180.

(34) Yaralioglu, G. G.; Degertekin, F. L.; Crozier, K. B.; Quate, C. F. *J. Appl. Phys.* **2000**, *87*, 7491.

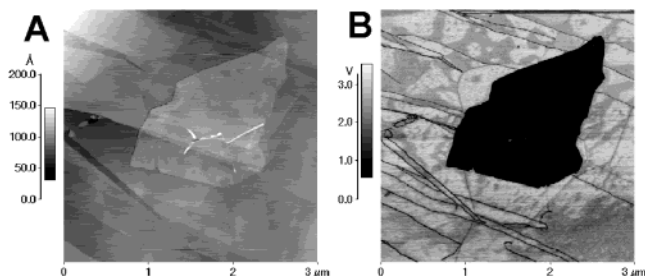


Figure 7. Force modulated microscopy of individual clay nanoplatelets on HOPG. (A) is the topology image, and (B) is the FMM image. In the FMM image, a darker shade indicates a lower vibration amplitude of the AFM tip, hence greater damping of the FMM signal.

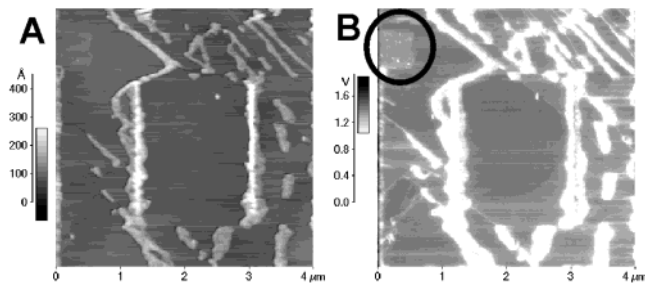


Figure 8. Sweeping of the impurity on a HOPG surface. (A) is a contact mode image, and (B) is a LFM image. The circle in the upper left-hand corner shows a single clay nanoplatelet.

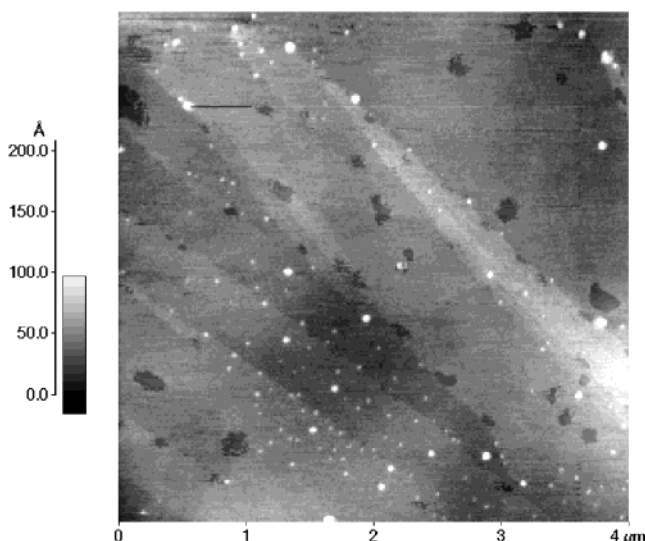


Figure 9. Tapping mode image of the clay impurities on HOPG.

baked sample difficult, as shown in Figure 8. In the figure there is one small clay nanoplatelet in the upper left-hand corner of the image; however, the impurity dominates the image. This image was preceded by several $2\ \mu\text{m}$ scans, which swept the impurities into two parallel lines. We found that the more that the clays are exfoliated (by increasing the amount of time the suspension is sonicated), the more impurity is found to be present in the water. In Figure 8, there are graphite step edges visible in the LFM image, and the impurities seem to be attracted to these edges and form lines. A tapping mode image of the impurity on HOPG, shown in Figure 9, shows that heating the sample drives the impurity to form a film that appears to be ordered. As observed in the contact mode images in Figure 8, the impurity is highly mobile on a graphite surface and tends to collect along step edges on the HOPG substrate.

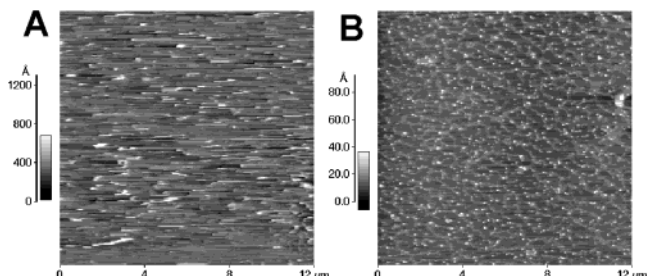


Figure 10. AFM contact mode topography images of the filtrate separated from the clay suspensions on mica. (A) was taken with an untreated tip. (B) was recorded with an AFM tip treated with dodecylamine and suggests that the impurity is hydrophilic.

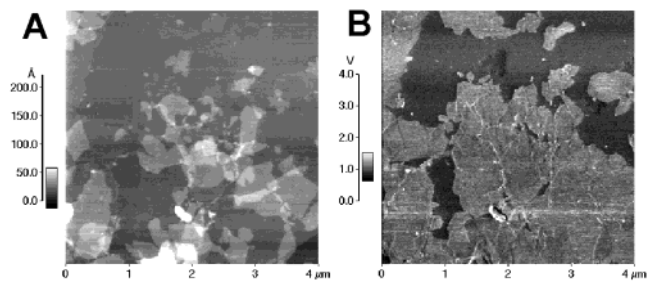


Figure 11. AFM image of clay sample ME-100 on mica. (A) is a contact mode topography image, and (B) is LFM. After drying, the friction is higher on the clays than the mica substrate.

To better understand the role that the impurity(ies) is (are) playing in our AFM images, a suspension of ME-300 was prepared. The ME-300 sample was filtered through a $0.20\ \mu\text{m}$ disk filter (Fisher #09-7190) so that most of the clays are removed, leaving just the impurity. Only a few drops of water passed through this filter before it was completely clogged. But this was enough that we could get data on concentrated impurities by AFM and TOF-SIMS. A drop of the filtrate was placed on a mica surface and allowed to dry. After drying, a film formed on the mica substrate as shown in Figure 10. It was almost impossible to scan in contact mode. However, after the AFM tip was treated with dodecylamine to reduce the capillary force,²¹ a much better image resulted (right image in Figure 10). This is consistent with the impurity being hydrophilic, as would be the case for a silicate or sodium hydroxide/water complex. Some of this filtrate was placed on a gold foil and analyzed via time-of-flight secondary ion mass spectrometry (TOF-SIMS). The elements and molecular fragments found by TOF-SIMS were consistent with those in the starting material, namely, sodium, fluorine, magnesium, and silicates.

The several different types of clay studied here were found to be very similar. For example, AFM images of the ME-100 sample suggest that the individual nanoplatelets in that sample are the same lateral size as those for the ME-300 sample (see Figure 11).³⁵ After the sample had dried for a day the lateral force image shows higher friction on the clay nanoplatelets than the mica substrate, suggesting that the ME-100 sample has a very similar surface chemistry, and comparable impurities, as the ME-300 sample.

Since impurities were found in all clay samples, tests were conducted to prove that the ultrasonic dispersion was not the source of the impurity due to breaking off of small parts of the clay nanoplatelets. Thus, a sample

(35) While manufacturer designations ME-100 and ME-300 are based on differences in light scattering behavior, we believe that the individual nanoplatelets comprising the clays are of similar size.

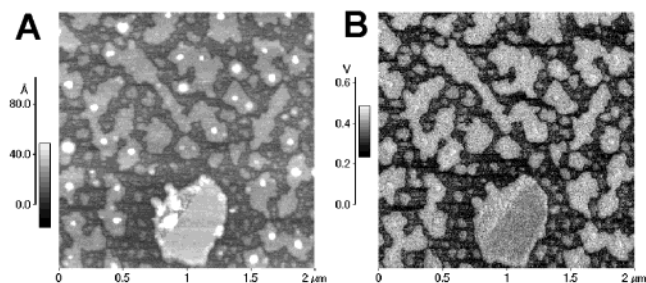


Figure 12. AFM image of clay exfoliated by stirring. (A) is the tapping mode topology image, and (B) is the phase image.

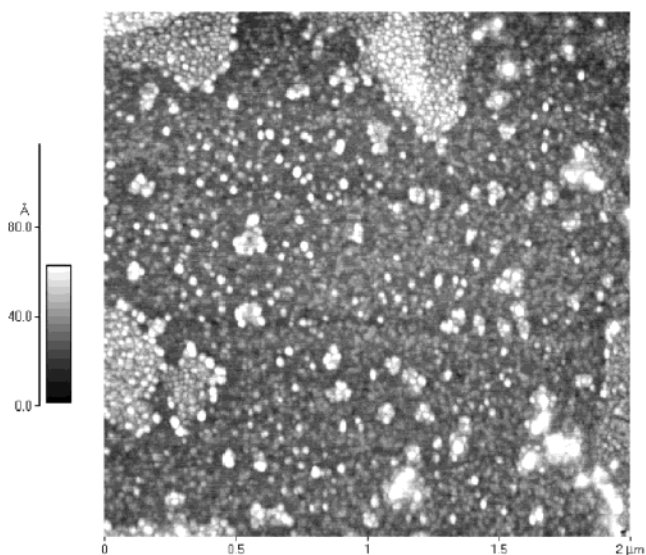


Figure 13. Tapping mode AFM image of sample of baked clay nanoplatelets on mica.

suspension was prepared by low-speed mechanical stirring using a magnetic stir bar. After a week of gentle stirring, the clays were well dispersed in water, but the impurity was also still present. A tapping mode image of a sample prepared in this way is shown in Figure 12. Note the ordering of the impurity. There is just one nanoplatelet in this image, in the lower center. The humidity was 50% when this image was recorded. When tapping mode is properly tuned, islands of water can be imaged;³⁶ thus, the islands imaged in Figure 12 are suspected to be mostly water. Also evident in the image are small spheres (diameters on the order of 5 nm) that are almost always seen in tapping mode images of the clays and, as discussed below, are believed to be sodium hydroxide.

At its core, AFM is a surface probe. Our results show that these impurities can completely dominate AFM measurements of the clay nanoplatelets and their properties. As a further investigation into these small spherical impurities, a sample of ME-300 was prepared and dried in an oven at 100 °C. Figure 13 is a tapping mode image recorded at very low humidity (less than 5%). Note the presence of many of the small spherical impurities. Because these spheres look very similar to potassium hydroxide particles noted by other researchers,^{37–39} we believe they are sodium hydroxide formed by the reaction of the original sodium intercalation ion with water. This hypothesis was tested by placing a drop of pure water on

the surface in Figure 13. After a minute, the water was flame tested and showed a bright orange flame indicative of sodium. After rinsing and repeating the flame test, no evidence of sodium was visible, which suggests that these mobile sodium ions were removed. After rinsing in water, the sample was checked again by AFM and the small spheres were largely gone.

Attempts To Separate the Clays from the Impurity. Numerous procedures to separate the nanoplatelets from the impurities have been attempted. While sedimentation is the obvious first choice, once exfoliated both the nanoplatelets and the associated impurities will stay suspended in water for an indefinite amount of time. Attempts to filter this nanoplatelet-impurity suspension were not successful, as the pores of the filter were instantly clogged by the nanoplatelets. Another method was to deposit the clays on a mica surface, followed by drying and subsequent rinsing with clean water; however, both the clays and the impurities remained on the substrate. Even when placed in boiling water for several hours, the impurities were not removed, indicating that at least one of the impurities is insoluble in water and cannot be removed from the substrate once dried.

Because the clay is stable to very high temperatures, attempts to drive off the impurities by heating the substrate were undertaken. Clays on mica were heated as high as 500 °C, but the impurities remained on the substrate. On glass, the clays were heated to a red heat in a propane flame; while the clays were burned off, the impurity still remained. As discussed earlier, dc electrophoresis as a means to separate the impurities from the clays was also ineffective; thus, any surface charge on the nanoplatelets is either very weak or screened in some way.

A chemical method to separate the impurities from the clay does not seem likely, as the water-insoluble impurity is probably a silicate and thus very similar to the clays themselves. However, an amine-terminated surface was tested in the hopes that the clay nanoplatelets would stick to the amine. The surface could then be washed before it dries and the impurity flushed away, leaving the clay behind. Our first attempt at this was to modify a mica surface with 3-aminopropyltriethoxysilane by placing several drops of the 3-aminopropyltriethoxysilane in various organic solvents and then dipping a freshly cleaved mica substrate into the solution for 1–5 min. Our technique is a simplification of a solution-based silane modification of silicon oxide surfaces reported by others.^{40,41}

Our results indicate that this method depends strongly on the solvent used to deposit the silane on the mica substrate. If toluene was used, a very flat (surface roughness less than 0.5 nm rms) hydrophobic surface resulted on the mica substrate, but it had almost no affinity for the clays. However, if ACN or DMF was used as the solvent, the clays strongly adhered to the substrate surface. Vigorous rinsing with pure water before the sample could dry did not remove the clay plates, suggesting that when ACN or DMF is used as solvent, the aminosilane is cross-linking and creating a surface with active silane groups exposed. Conceivably, these silanes then react with the clays and bind them to the surface through a covalent bond. Unfortunately, any excess silanes at the surface also tend to react strongly with the AFM tip. In Figure

(36) Gil, A.; Colchero, J.; Luna, M.; Gomez-Herrero, J.; Baro, A. M. *Langmuir* **2000**, *16*, 5086.

(37) Xu, L.; Salmeron, M. *Langmuir* **1998**, *14*, 5841.

(38) Rieutord, F.; Salmeron, M. *J. Phys. Chem. B* **1998**, *102*, 3941.

(39) Hu, J.; Carpick, R. W.; Salmeron, M.; Xiao, X. D. *J. Vac. Sci. Technol. B* **1996**, *14*, 1341.

(40) Foisner, J.; Glaser, A.; Kattner, J.; Hoffmann, H.; Friedbacher, G. *Langmuir* **2003**, *19*, 3741.

(41) Kitaev, V.; Seo, M.; McGovern, M. E.; Huang, Y.; Kumacheva, E. *Langmuir* **2001**, *17*, 4274.

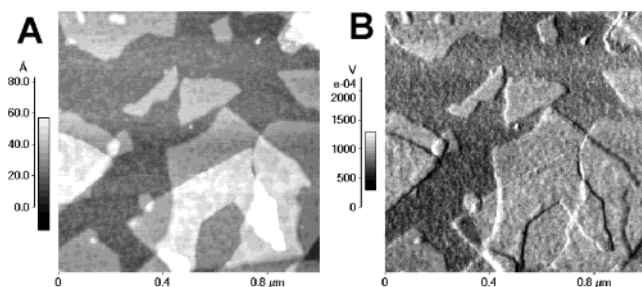


Figure 14. AFM image of amine-treated clay sample. (A) is a tapping mode image, and (B) is the phase image.

14, a tapping mode AFM image shows a large numbers of clays strongly bound to a mica substrate. Contact mode images were impossible to obtain, since silanes react strongly with silicon nitride AFM tips. This precludes obtaining detailed information about the impurities using this method.

Conclusions

In summary, several different exfoliated clays were studied. The individual clay nanoplatelets are approximately $1\ \mu\text{m}$ in the lateral direction and $1\ \text{nm}$ thick. These clay nanoplatelets are extraordinarily compliant and readily conform to nanoscale surface features. In the process of imaging these nanoplatelets, we found that the clay sheets have substantial quantities of mobile impurities that could not be separated from the clay nanoplatelets. Because AFM is a surface probe, these impurities interfere with precise AFM measurements, especially FMM, of the individual clay sheets. The impurities are of two types; one is water-soluble and appears to be sodium

and perhaps its counterions. The other impurity is silicate-based and water-insoluble and is mobile on an atomically smooth surface. The precise nature and chemistry of these impurities are currently unknown and the focus of additional study in our lab.

The presence of the impurities, and the inability to separate them from the clay nanoplatelets, is significant and will impact the use of clay nanoplatelets in applications. For example, because of their nanometer size, these impurities will contribute a large surface area component to a composite system as well as influence the interaction of the clay nanoplatelets with the matrix. The presence of these impurities will also interfere with nanoscale measurements of the stiffness of a single clay sheet and is undesirable for applications where the nanoplatelets are to be used as a building block for molecular electronic systems. It is our hope that this paper will stimulate further interest in clay nanoplatelets and that an awareness of the presence of these impurities will lead to the development of rigorous clay purification methods.

Acknowledgment. The authors thank Emmanuel P. Giannelis and Daniel Schmidt for materials and advice. We gratefully acknowledge the grant support from the Office of Naval Research Mechanics of Nanostructures grant under Award No. N000140210870, the NASA University Research, Engineering and Technology Institute on Bio Inspired Materials (BIMat) under Award No. NCC-1-02037, and the NASA Langley Research Center Computational Materials: Nanotechnology Modeling and Simulation Program.

LA0347814